of approximately 0.2 mol must be contributed from the weakly proton-linked reactions of L and K_S^T. In the presence of 20 mM Phe, the initial binding of Phe to the T state would lead to an absorption of 0.35 mol of proton. Subsequent titration of the system with substrate would lead to a state change and in the release of Phe (Figure 4B). These two reactions can account for 0.6 mol of the observed 0.8 mol of proton released. Thus, by considering the quantitative proton linkages among these equilibrium constants, it is possible to provide a rationale for the kinetic behavior of PK in solution.

In summary, the synergistic effect of Phe and proton on the kinetic behavior of muscle PK is the composite effects of proton on the multiple equilibria governing the regulatory mechanism of the enzyme. The strong and negative proton linkage observed in the binding affinity of Phe for the inactive T state seems to play a major role.

ACKNOWLEDGMENTS

The critical review and stimulating discussion with Dr. Tomasz Heyduk are greatly appreciated.

Registry No. PK, 9001-59-6; PEP, 138-08-9; ADP, 58-64-0; L-Phe, 63-91-2; H^+, 12408-02-5.

REFERENCES

Boyer, P. D. (1962) *Enzymes, 2nd Ed. 6*, 95.
Bucher, T., & Pfleiderer, G. (1955) *Methods Enzymol. 1*, 435–440.
Consler, T. G., & Lee, J. C. (1988) *J. Biol. Chem. 263*, 2787–2793.
Consler, T. G., Uberbacher, E. C., Bunick, G. J., Liebman, M. N., & Lee, J. C. (1988) *J. Biol. Chem. 263*, 2794–2801.
Consler, T. G., Woodward, S. H., & Lee, J. C. (1989) *Biochemistry 28*, 8756–8764.
Cornish-Bowden, A. (1979) in *Fundamentals of Enzyme Kinetics*, Chapter 6, p 99, Butterworths, London.
Dougherty, T. M., & Cleland, W. W. (1985a) *Biochemistry 24*, 5870–5875.
Dougherty, T. M., & Cleland, W. W. (1985b) *Biochemistry 24*, 5875–5880.
Gregory, R. B., & Ainsworth, S. (1981) *Biochem. J. 195*, 745–751.
Hill, A. V. (1910) *J. Physiol. (London) 40*, 190–224.
Hirose, M., & Kano, Y. (1971) *Biochim. Biophys. Acta 251*, 376–379.
Kayne, F. J., & Suelter, C. (1965) *J. Am. Chem. Soc. 87*, 897–900.
Kayne, F. J., & Suelter, C. (1968) *Biochemistry 7*, 1678–1684.
Kayne, F. J., & Price, N. C. (1972) *Biochemistry 11*, 4415–4420.
Kwan, C. Y., & Davis, R. C. (1980) *Can. J. Biochem. 58*, 188–193.
Mildvan, A. S., & Cohn, M. (1965) *J. Biol. Chem. 240*, 238–246.
Mildvan, A. S., & Cohn, M. (1966) *J. Biol. Chem. 241*, 1178–1193.
Monod, J., Wyman, J., & Changeaux, J. P. (1965) *J. Mol. Biol. 12*, 88–118.
Oberfelder, R. W. (1982) Ph.D. Thesis, Department of Biochemistry, St. Louis University.
Oberfelder, R. W., Lee, L. L.-Y., & Lee, J. C. (1984a) *Biochemistry 23*, 3813–3821.
Oberfelder, R. W., Barisas, B. G., & Lee, J. C. (1984b) *Biochemistry 23*, 3822–3826.
Phillips, F. C., & Ainsworth, S. (1977) *Eur. J. Biochem. 8*, 729–735.
Wyman, J. (1964) *Adv. Protein Chem. 19*, 224–285.

Structure and Polymorphism of Saturated Monoacid 1,2-Diacyl-*sn*-glycerols†

Dharma R. Kodali, David A. Fahey, and Donald M. Small*
Department of Biophysics, Boston University School of Medicine, Housman Medical Research Center, 80 East Concord Street, Boston, Massachusetts 02118-2394

Received April 18, 1990; Revised Manuscript Received August 14, 1990

ABSTRACT: The 1,2-diacyl-*sn*-glycerols (1,2-DGs) are the predominant naturally occurring isomer found in cell membranes, lipid droplets, and lipoproteins. They are involved in the metabolism of monoacylglycerols, triacylglycerols, and phospholipids. The 1,2-DGs participate in the activation of protein kinase C, in phosphorylation of target proteins, and in transduction of extracellular signals into the cell. We have undertaken a study of the physical properties of a homologous series of synthetic optically active diacylglycerols. Stereospecific 1,2-diacyl-*sn*-glycerols were synthesized with saturated fatty acyl chains of 12, 16, 18, 22, and 24 carbons in length. Their polymorphic behavior was examined by differential scanning calorimetry and X-ray powder diffraction. The solvent-crystallized form for all the 1,2-DGs packs in the orthorhombic perpendicular subcell (β') and melts with a single sharp endotherm to an isotropic liquid. On quenching, the C_{12}, C_{16} and C_{18} compounds pack in a hexagonal subcell (α), whereas the C_{22} and C_{24} pack in a pseudohexagonal subcell (sub-α). The sub-α phase reversibly converts to the α phase. The long spacings of these compounds in both the α and β' phases increase with chain length. In the α and β' phases, the acyl chain tilts were found to be 90° and 62° from the basal methyl plane. The polymorphic behavior of 1,2-diacyl-*sn*-glycerol is quite different from that of the corresponding monoacid saturated 1,3-diacylglycerols which form two β phases with triclinic parallel subcells.

Diacyl-*sn*-glycerols (DGs) are comprised of two fatty acyl chains esterified to two out of three glycerol carbons. Due to the prochiral nature of the glycerol molecule, esterification of two acyl chains of the same kind results in three isomeric 1,2-, 2,3-, and 1,3-diacyl-*sn*-glycerols (IUPAC–IUB, 1977). The racemic 1,2-diacyl-glycerols are a mixture of 1,2- and 2,3-diacyl-*sn*-glycerols. In this study, the racemic forms are

†Supported by grants from the National Institutes of Health (HL26335 and HL0729).

0006-2960/90/0429-10771$02.50/0

indicated as racemic, and the others are optically active forms. Naturally occurring DGs are the 1,2-isomers and often contain a saturated acyl chain at the 1-position and an unsaturated acyl chain at the 2-position.

1,2-Diacyl-*sn*-glycerol (1,2-DG) is a neutral, moderately amphipathic, ubiquitous isomeric form that participates in the biosynthesis of triacylglycerols (TGs), monoacylglycerols (MGs), phosphatidic acid (PA), and other phospholipids (PLs). In the final step of TG synthesis, the enzyme diacylglycerol acyltransferase esterifies an activated fatty acid to the 3-position of 1,2-DG. Cytidinediphosphoethanolamine (CDP-ethanolamine) and CDP-choline are utilized by phosphoethanolamine transferase or phosphocholine transferase, respectively, to transfer the head groups to 1,2-DG in the final step of phosphatidylethanolamine (PE) and phosphatidylcholine (PC) synthesis via the salvage pathway. 1,2-DG can be phosphorylated to PA by DG kinase which is then transformed to cytidinediphosphodiacylglycerol (CDP-DG) by PA–cytidyl transferase utilizing cytidine triphosphate (CTP). CDP-DG is a precursor of phosphatidylserine (PS), phosphatidylinositol (PI), and phosphatidylglycerol. In addition to anabolic reactions, DG is a substrate for DG lipase which cleaves a fatty acid (FA), leaving monoacylglycerol (MG). The cleaved FA is often arachidonic acid which is precursor of prostaglandins and leukotrienes. The role of 1,2-DG in the phosphoinositide cycle is reviewed elsewhere (Sekar & Hokin, 1986). As an activator of protein kinase C, 1,2-DG also participates in the transduction of extracellular signals across the plasma membrane (Nishizuka, 1986). It has been shown that 1,2-DG is the only isomer capable of activating protein kinase C (Rando et al., 1984; Ganong et al., 1986).

In view of the recently recognized importance of 1,2-DG, we have undertaken a systematic study of the physical properties of a homologous series of synthetic optically active diacylglycerols, using differential scanning calorimetry (DSC) and X-ray diffraction. There have been relatively few reported physical studies of 1,2-diacyl-*sn*-glycerols. A powder diffraction study of 1,2-dipalmitoyl-*sn*-glycerol was presented by Dorset et al. in 1978, and Pascher et al. reported the crystal structure of the β' form of 1,2-dilauroyl-*sn*-glycerol in 1981. The physical studies of racemic 1,2-diacylglycerols include a study of the α form of dipalmitin (Dorset, 1974) and an X-ray diffraction study of a C_{12} through C_{18} even-carbon series (Howe & Malkin, 1951). Recently, Dorset and Pangborn (1988) reported a single-crystal structure of the β' form and the structure of an epitaxially grown α form of 1,2-dipalmitoyl-*sn*-glycerol; the β' form structure of this compound is isostructural to that of 1,2-dilauroyl-*sn*-glycerol (Pascher et al., 1981). Similar to that of triacylglycerols (TGs), the DGs also exhibit polymorphic behavior [review by Chapman (1962) and Small (1986)]. The racemic 1,2-isomers show a stable form with a β' subcell and a metastable α form (Howe & Malkin, 1951). The 1,3-isomer of saturated DGs shows a stable polymorphic form with a β subcell and a lack of any observable α form (Baur et al., 1949). The single-crystal structures of two heavy-atom-substituted saturated 1,2-DGs (Larsson, 1963; Hybl & Dorset, 1971) have been solved. Though there have been several physical studies of symmetrical unsaturated 1,3-diacylglycerols (Daubert & Lutton, 1947; Carter & Malkin, 1947; Daubert & Sidhu, 1948; O'Connor et al., 1955; Gros & Feuge, 1957), there have been no reported physical studies of pure mono- or diunsaturated 1,2-diacylglycerols. Since these are the biologically occurring DG species, the lack of physical studies is surprising. However, the problem of acyl migration during synthesis and handling has likely impeded progress in this area, especially for unsaturated 1,2-DGs. The preparation and handling of the 1,2-isomer must be monitored carefully since acyl migration can occur, even in the solid state, producing the 1,3-isomer (Dorset et al., 1978; Lok & Ward, 1985). The results of a systematic study of the acyl migration occurring in these compounds have been presented (Kodali et al., 1990).

In the present paper, systematic thermal and X-ray diffraction studies of a homologous series of monoacid 1,2-diacyl-*sn*-glycerols with even-carbon saturated acyl chains of 12, 16, 18, 22, and 24 carbons in length are presented. The studies were carried out under conditions where acyl migration was minimal. Monoacid 1,3-diacylglycerols with even-carbon saturated acyl chains of 16 and 18 carbons in length are studied for comparison.

Materials and Methods

Synthesis and Purity. Stereospecific monoacid 1,2-diacyl-*sn*-glycerols were synthesized with saturated acyl chains of 12, 16, 18, 22, and 24 carbons in length. In brief, the 1,2-diacyl-*sn*-glycerols are synthesized from 1,2-diacyl-3-benzyl-*sn*-glycerols by debenzylation with dimethylboron bromide. The 1,2-diacyl-3-benzyl-*sn*-glycerols are prepared by esterification of 3-benzyl-*sn*-glycerol with 2 mol of appropriate fatty acid (Kodali et al., 1984). In the final step, the protecting benzyl group from the 1,2-diacyl-3-benzyl-*sn*-glycerols is removed by treating with excess (2.5 mol) dimethylboron bromide. The usual workup of the reaction gave pure 1,2-diacyl-*sn*-glycerol without any 1,3-isomer. The detailed synthetic procedure for debenzylation by dimethylboron bromide will be published elsewhere. The purities of the compounds are checked by TLC and NMR (Serdarevich, 1967) and were found to be >99% pure. The 1,2-dipalmitoyl-*sn*-glycerol stored at −10 °C for a year contained less than 2% of 1,3-isomer. The symmetric 1,3-DGs are synthesized according to the literature procedure (Bentley & McCrae, 1970). At higher temperatures or in acidic or basic conditions, acyl migration can readily occur in diacylglycerols, forming unwanted isomers. The extent of acyl migration was carefully monitored by thin-layer chromatography (TLC) during synthesis and storage and after physical experiments (Kodali et al., 1990). TLC analysis of diacylglycerol purity was done on silica gel "G" plates in a solvent system consisting of chloroform/acetone, 96/4 (v/v). This solvent system resolved 1,2-isomers from 1,3-isomers and visualized by charring after spraying with dilute sulfuric acid. The charred plates were analyzed densitometrically, and an estimate of acyl migration was made (Kodali et al., 1990). Experimental protocols were designed to minimize acyl migration.

Physical Methods. Differential scanning calorimetry (DSC) was carried out on a Perkin-Elmer DSC-2 (Norwalk, CT). Approximately 2 mg of each compound, weighed to the nearest 0.01 mg, was sealed in a stainless-steel pan. An empty pan was used as a reference sample. Heating and cooling rates were 5 °C/min unless otherwise specified.

Experimental Protocol. Acylglycerols exhibit polymorphism due to different chain packing arrangements of similar lattice energy. Subtle differences in chain packing can be produced by varying the thermal history of the acylglycerols. Thus, it is essential that a precise thermal history be noted in DSC investigations. The general thermal protocol is as follows: (1) The solvent-crystallized DG was heated to approximately 10 °C above the melting endothermic peak temperature (T_f) corresponding to the transition to isotropic liquid. (2) The DG was then cooled to between 50 and 100 °C below T_f, and the peak temperature of the recrystallization exotherm, T_c, was

Table I: Thermodynamic Data from DSC Analysis of 1,2-Diacyl-*sn*-glycerols

acyl substituent	T_f[a] (°C)	ΔH_f[b] (kcal/mol)	ΔS_f[c] [cal/(mol·K)]	T_c[d] (°C)	ΔH_c,[e] (kcal/mol)	$T_{f\alpha}$[f] (°C)	$\Delta H_{f\alpha}$[g] (kcal/mol)	$\Delta S_{f\alpha}$[h] [cal/(mol·K)]
lauroyl (C_{12})[j]	47.5	19.0	59.3	15.1	8.8	19.5	8.8[i]	30.1[i]
palmitoyl (C_{16})[j]	70.1	28.3	82.5	47.3	15.2	51.3	14.6	45.0
stearoyl (C_{18})[j]	77.2	30.6	87.4	56.8	17.4	61.6	16.8	50.2
behenoyl (C_{22})[k]	85.7	39.7	110.7	69.5	22.9	73.3	22.9	66.1
lignoceroyl (C_{24})[k]	87.6	39.3	109.0	73.6	23.6	77.3	24.4	69.6

[a] Temperature of melting of β' phase, transition peak values. [b] Enthalpy of melting transition of β' phase. [c] Entropy of melting transition of β' phase, calculated from the enthalpy of melting. [d] Temperature of crystallization, transition peak values. [e] Enthalpy of crystallization. [f] Temperature of melting of α phase, transition peak values. [g] Enthalpy of melting of α phase. [h] Entropy of melting of α phase, calculated from the enthalpy of melting. [i] Calculated from the enthalpy of the crystallization exotherm of the α phase on cooling. [j] Means of two separate runs which differed by less than 0.5 °C for transition temperatures and less than 3% for enthalpy values. [k] Means of four separate runs. The maximum difference in transition temperatures was 0.5 °C. The ΔH_f for C_{22} was 39.7 ± 0.5 kcal/mol (mean ± standard error of mean, $n = 4$) and for C_{24} 39.3 ± 0.5 kcal/mol. The other thermodynamic values showed similar small dispersions from the mean values given in the table.

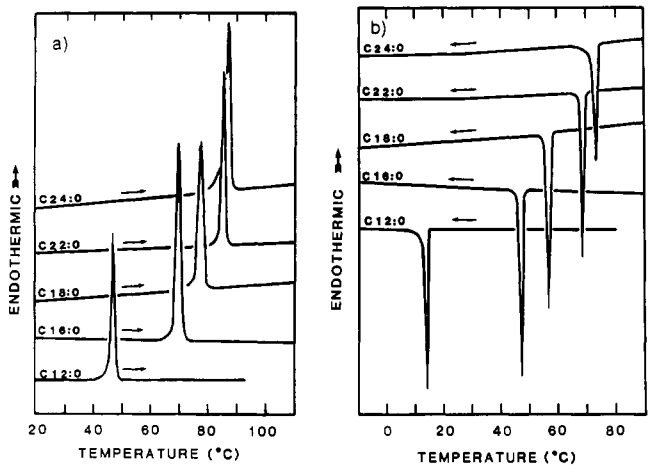

FIGURE 1: Heating and cooling transition of monoacid saturated 1,2-diacyl-*sn*-glycerols (1,2-DGs). (a) DSC initial heating (→) curves of hexane-crystallized 1,2-DG. Each diacylglycerol melts to an isotropic liquid with a single sharp endotherm. (b) DSC cooling (←) curves from the isotropic liquid of 1,2-DG. Each diacylglycerol exhibits a single sharp recrystallization exotherm. The chain lengths are indicated on the left of each tracing. The temperatures of the melting transitions (T_f) and crystallization transitions (T_c) and the thermodynamic values (ΔH and ΔS) are given in Table I.

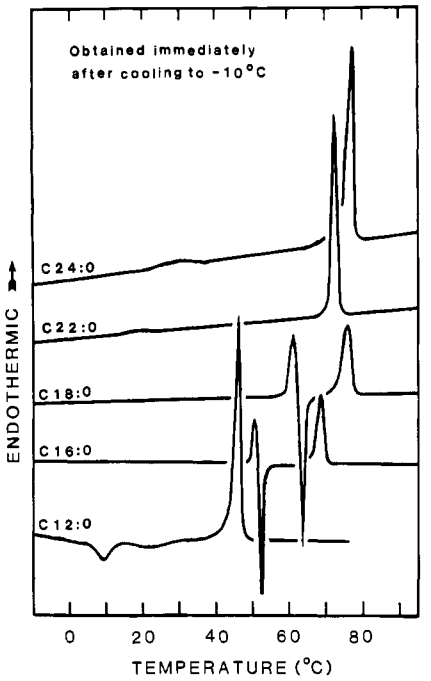

FIGURE 2: DSC second heating curves of saturated monoacid 1,2-diacyl-*sn*-glycerols immediately after cooling the melt to −10 °C.

obtained. (3) The DG was reheated after approximately 2 min required for data processing, and the immediate second heating was obtained. (4) To observe the thermal behavior of metastable forms, the 1,2-diacylglycerols were cooled to 5–10 °C below T_c and then reheated with or without incubation. The incubation period allowed polymorphic transitions to occur which were reflected in reheating scans.

The areas under the endotherms and exotherms were measured by planimetry to calculate the enthalpies of fusion (ΔH_f) and enthalpies of crystallization (ΔH_c) by comparing with a known standard enthalpy (indium). The estimated error margin for the indium standard is less than 0.5 °C (three separate samples) in the transition temperature and less than 2% (three runs) in enthalpy.

X-ray powder diffraction patterns of each sample were recorded using nickel-filtered Cu K_α radiation from an Elliot GX-6 (Elliot Automation, Borehamwood, U.K.) rotating-anode generator equipped with cameras employing Franks double-mirror optics (Franks, 1958) and toroidal mirror optics. In special cases, a Luzzati-Baro camera modified to incorporate single-mirror focusing and a Tennelec PSD 1100 position-sensitive detector (Tennelec, TN) were also used. The acylglycerols were packed into 1-mm-diameter Lindeman capillaries (Charles Supper, Natick, MA), sealed, and examined in variable-temperature sample holders. Diffraction was recorded for the solvent-crystallized form and for the melt-crystallized form at various temperatures between 0 and 90 °C. To correlate the structural changes with calorimetric events, 15–30-min acquisitions were taken on the position-sensitive detector at 10 °C intervals.

Results

Thermotropic Polymorphism. Figure 1a shows the DSC heating curves of the hexane-crystallized form of a series of saturated 1,2-diacyl-*sn*-glycerols. Each DG exhibits a single sharp endotherm corresponding to the transition to isotropic liquid. Figure 1b shows the DSC cooling curves. Each DG exhibits a single sharp recrystallization exotherm. Each compound undercooled to different extents ranging from 14 °C for the C_{24} DG to 33 °C for the C_{12} DG. While it is difficult to appreciate on Figure 1b, C_{22} and C_{24} underwent a very broad low-enthalpy exotherm in the region of 10–40 °C. These exothermic transitions appear as a slight change in the shape of the baseline. The transition temperature values at the endothermic (Figure 1a) peaks, T_f, and exotherm (Figure 1b) minima, T_c, are given in Table I. The thermodynamic data obtained from the DSC curves, enthalpies of fusion, ΔH_f, enthalpies of crystallization, ΔH_c, and entropy change upon melting, ΔS_f, are also tabulated.

The immediate second heating curves for these compounds are shown in Figure 2. Upon reheating, the C_{12} DG undergoes

Table II: X-ray Powder Diffraction Long and Short Spacings of Saturated Monoacid 1,2-Diacyl-*sn*-glycerols Crystallized from Hexane

	acyl substituent				
	lauroyl, 12:0	palmitoyl, 16:0	stearoyl, 18:0	behenoyl, 22:0	lignoceroyl, 24:0
long spacings[a] (Å)	34.4 (s), 1	43.4 (s), 1	47.9 (s), 1	57.0 (vs), 1	61.7 (vs), 1
	17.0 (vw), 2	22.1 (m), 2	23.9 (w), 2	28.4 (w), 2	30.8 (w), 2
	11.5 (m), 3	14.5 (m), 3	15.9 (m), 3	19.0 (m), 3	20.5 (m), 3
	8.7 (m), 4	10.8 (w), 4			
	6.9 (w), 5			11.4 (w), 5	12.4 (w), 5
		7.3 (m), 6	8.0 (w), 6	9.5 (w), 6	
		6.6 (w)	6.8 (w)	7.0 (w)	
	6.3 (w)	6.2 (w)	6.4 (w)	6.2 (w)	
	5.7 (w)	5.8 (w)	5.9 (w)		
		5.3 (w)	5.4 (w)	5.4 (w)	
	5.2 (w)	5.2 (w)	5.2 (w)	5.1 (w)	
		5.0 (w)		4.88 (w)	4.98 (w)
		4.73 (w)	4.73 (w)	4.70 (w)	4.71 (w)
short spacings (Å)			4.46 (w)	4.45 (m)	4.50 (m)
	4.38 (m)	4.42 (m)	4.42 (w)	4.38 (w)	4.38 (w)
		4.28 (m)	4.28 (m)	4.27 (m)	4.26 (m)
		4.13 (m)		4.13 (w)	4.14 (w)
	4.04 (s)	4.02 (s)	4.04 (s)	4.05 (s)	4.06 (s)
	3.82 (m)	3.89 (m)			3.90 (w)
		3.75 (m)	3.75 (m)	3.75 (m)	3.73 (m)
	3.49 (w)	3.50 (w)			
		3.32 (w)			

[a] The estimated intensities are given in parentheses: strong (s), medium (m), weak (w), very (v). The order of 0,0,l reflection is indicated after the diffraction long spacing intensity.

an exothermic polymorphic transition at about 10 °C, followed by melting at 46.5 °C, which is close to the hexane-crystallized form melting temperature. In contrast, upon reheating, the C_{16} and C_{18} diacylglycerols undergo low-temperature melting of the α form at a temperature, $T_{f\alpha}$, tabulated in Table I. This low-melting form immediately recrystallized to a form which melted within 1 °C of the hexane-crystallized form melting temperature. Upon reheating, the C_{22} and C_{24} DGs revealed a broad low-enthalpy endotherm (<2 kcal/mol) at 19 and 30 °C, respectively. These endotherms are polymorphic transitions corresponding to the very broad exotherms found in Figure 1b. Further heating produced sharp melting endotherms at 73 and 77 °C for the C_{22} and C_{24} DGs, respectively. These temperatures are 12 and 10 °C below the hexane-crystallized form melting temperatures, respectively, and are given as α-form melting temperatures, $T_{f\alpha}$, in Table I.

A single melting endotherm at $T_{f\alpha}$ can be obtained for the C_{16} and C_{18} DGs if they are cooled to just below T_c and immediately reheated. This behavior is shown for the C_{16} DG after cooling to 41 °C in Figure 3a,b. Melting enthalpies and entropies for the α form of the C_{16} and C_{18} DGs given in Table I were obtained from these curves. If the C_{16} DG is cooled to 41 °C and incubated for various times, an additional endotherm at 68.5 °C appears with enthalpy proportional to incubation time (Figure 3c,d). This indicated the nucleation and growth of a higher melting polymorph during storage at 41 °C. Acyl migration is not the cause, since this endotherm does not correspond to the 1,3-DG melting temperature (74.9 °C) and the amount of 1,3-DG that forms after 0.5 h at 41 °C is extremely small (<2%).

The hexane-crystallized 1,3-dipalmitoylglycerol melted with a single sharp endotherm with a peak temperature of 74.9 °C. On cooling, recrystallization occurred at 65.5 °C, and upon reheating, the compound melted at 73.4 °C. This melting temperature is about 1.5 °C below the melting temperatures of the hexane-crystallized form. In an attempt to observe α-form melting, the sample was rapidly cooled to just below T_c and immediately reheated, but no evidence of α-form melting was observed. The 1,3-distearoylglycerol behaved similarly; the hexane-crystallized form melted to an isotropic liquid at 78.4 °C. On cooling, the compound recrystallized at 69.1 °C and upon reheating melted at 77.8 °C.

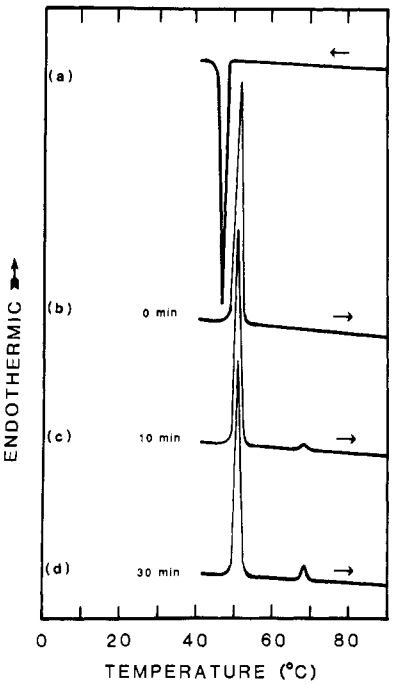

FIGURE 3: DSC cooling (←) and heating (→) curves of 1,2-dipalmitoyl-*sn*-glycerol (C_{16}-DG). (a) The sample from the isotropic liquid is cooled to 41 °C [6 °C below the crystallization (T_c) of the α phase] and (b) immediately reheated. A single endotherm corresponding to α-form melting is obtained. If the sample is held at 41 °C for (c) 10 min or (d) 30 min, reheating produces an additional endotherm at 68.5 °C with the enthalpy proportional to the incubation time, indicating nucleation and growth of the β' form.

Crystal Structure and X-ray Powder Diffraction. Table II lists the *d* spacings derived from powder diffraction of the hexane-crystallized form of the C_{12}, C_{16}, C_{18}, C_{22}, and C_{24} saturated monoacid 1,2-diacyl-*sn*-glycerols. Up to 6 orders of 0,0,L reflections could be indexed. The $d_{0,0,1}$ diffraction was strong, and $d_{0,0,3}$ diffraction was of medium intensity for all members of the series. The short spacing region showed

Table III: X-ray Powder Diffraction Long and Short Spacings of Saturated Monoacid 1,2-Diacyl-*sn*-glycerols after Quenching Isotropic Liquid to between −5 and 5 °C

	acyl substituent				
	lauroyl,[a] 12:0	palmitoyl,[b] 16:0	stearoyl,[a] 18:0	behenoyl,[a] 22:0	lignoceroyl,[a] 24:0
long spacings[c] (Å)	37.4 (vs), 1		54.3 (vs), 1	62.8 (vs), 1	67.9 (s), 1
	19.0 (w), 2	24.7 (w), 2	27.2 (w), 2		34.3 (w), 2
	12.5 (m), 3	16.5 (s), 3	18.1 (m), 3	21.2 (m), 3	22.7 (m), 3
	9.4 (w), 4	12.3 (w), 4	13.5 (w), 4		17.3 (w), 4
				12.9 (w), 5	13.7 (w), 5
		8.1 (w), 6	9.1 (w), 6	10.6 (w), 6	11.6 (w), 6
short spacings (Å)	4.11 (s)	4.13 (s)	4.15 (s)	4.13 (s)	4.14 (s)
				3.78 (m)	3.79 (m)

[a] Data obtained with position-sensitive detector. [b] Data obtained with torroidal camera. [c] The estimated intensities are shown in parentheses: very strong (vs), strong (s), medium (m), and weak (w). The order of 0,0,l reflection is indicated after the diffraction long spacing intensity.

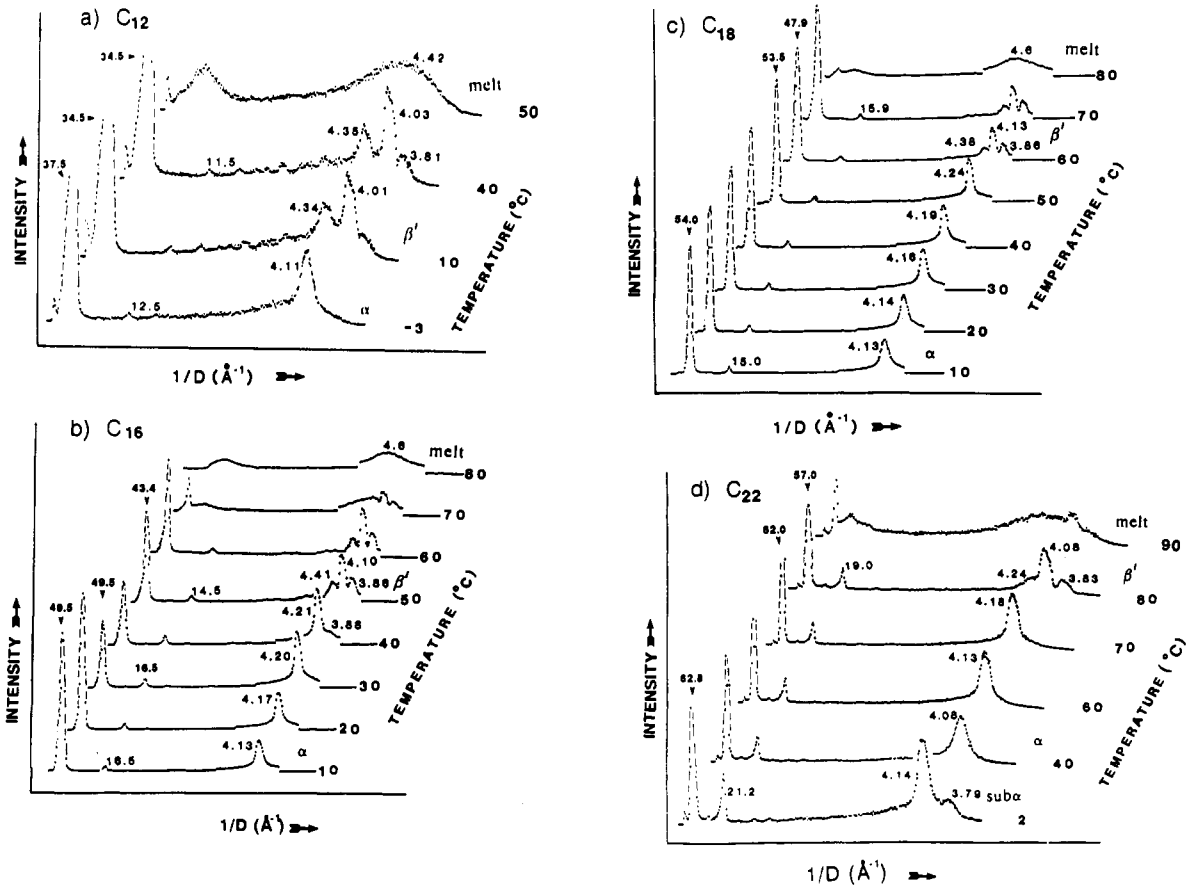

FIGURE 4: X-ray diffraction patterns of various 1,2-diacyl-*sn*-glycerols recorded on a position-sensitive detector. The numbers next to diffraction maxima refer to the corresponding *d* spacings in angstroms. (a) 1,2-Dilauroyl-*sn*-glycerol (C_{12}) while heating from −3 to 50 °C. Structural changes occur between −3 and 10 °C, indicated by α to β' short spacing changes, and a decrease in the long spacing from 37.5 to 34.5 Å. All sharp reflections disappear on melting. (b) 1,2-Dipalmitoyl-*sn*-glycerol (C_{16}) while heating from 0 to 80 °C. Structural changes occur between 40 and 50 °C, indicated by α to β' short spacing changes and a decrease in the long spacing from 49.5 to 43.4 Å. (c) 1,2-Distearoyl-*sn*-glycerol (C_{18}) while heating from 0 to 80 °C. Structural changes occur between 50 and 60 °C, indicated by α to β' short spacing changes and a decrease in the long spacing from 54.0 to 47.9 Å. (d) 1,2-Dibehenoyl-*sn*-glycerol (C_{22}) while heating from 2 to 90 °C. Structural changes occur between 2 and 40 °C, as seen by changes from sub-α short spacings (ca. 4.1 and 3.8 Å) to an α-form short spacing (ca. 4.1 Å) but without change in long spacing. Structural changes occur between 70 and 80 °C, indicated by α to β' short spacing changes and a decrease in long spacing from 62.0 to 57.0 Å. Melting is nearly complete at 90 °C.

medium to strong diffraction at ca. 4.3, 4.05, and 3.75 $Å^{-1}$ for all members of the series. Medium-intensity diffraction at ca. 4.45 $Å^{-1}$ also occurred for the C_{16}, C_{22}, and C_{24} diacylglycerols.

Table III lists the *d* spacings for each 1,2-diacyl-*sn*-glycerol, after rapidly cooling the isotropic liquid to about 0 °C. The first order for C_{16} 1,2-DG is not reported in Table III because it could not be measured from the toroidal camera film. However, the PSD data (Figure 4b) indicate a first-order diffraction of 1/49.5 $Å^{-1}$. For these compounds, the long spacings increase linearly with chain length. The first- and third-order diffractions are strong to medium in all members of the series. The wide-angle region shows a single strong diffraction ca. 4.1 $Å^{-1}$ for the C_{12}, C_{16}, C_{18} diacylglycerols. In contrast, two strong to medium reflections at ca. 4.14 and 3.78 $Å^{-1}$ were observed for the C_{22} and C_{24} diacylglycerols.

X-ray analysis of the 1,2-diacyl-*sn*-glycerols as a function of temperature was carried out with the position-sensitive detector. In order to correlate structural changes with calorimetric events, 15–30-min acquisitions were taken at 10 °C intervals as the samples were heated from 0 °C. Figure 4a

shows diffraction patterns of the C_{12} diacylglycerol at −3, 10, 40, and 50 °C. Structural changes occur between −3 and 10 °C, indicating the transformation of α to β' phase. The β'-phase melting is complete at 50 °C. Panels b and c of Figure 4 show diffraction patterns at 10 °C intervals between 10 and 80 °C for the C_{16} and C_{18} 1,2-DGs, respectively. The wide-angle diffractions that occur between 40 and 50 °C for the C_{16} DG and between 50 and 60 °C for the C_{18} DG show the α to β' transformation. At 80 °C, melting is complete for the C_{16} DG and nearly complete for the C_{18} DG. Figure 4d shows diffraction patterns for the C_{22} DG at 2, 40, 60, and 70, 80, and 90 °C. Structural changes in the wide-angle region occur between 2 and 40 °C without changes in long spacing, indicating a sub-α to α transition. The transformation of the α phase to the β' phase occurs between 70 and 80 °C. Melting is nearly complete at 90 °C. The diffraction patterns of C_{24} DG show structural changes between 20 and 40 °C without changes in long spacing, indicating the transformation of the sub-α form to the α form (data not shown). The α to β' transition occurs around 80 °C.

The powder diffraction d spacings for the hexane-crystallized and melt-crystallized 1,3-dipalmitoylglycerol and 1,3-distearoylglycerol are recorded. The long spacing for the hexane-crystallized forms (C_{16}, 48 Å; C_{18}, 52 Å) are 2–3 Å greater than the melt-crystallized forms (C_{16}, 45 Å; C_{18}, 50 Å). The wide-angle reflection of these compounds in both the forms shows the strongest diffraction at ca. 1/4.6 Å^{-1}, indicating β-subcell packing in both the hexane-crystallized and melt-crystallized forms.

Discussion

1,2-Diacyl-sn-glycerols. The melting transition temperatures of the β' form ($T_{f\beta'}$), the crystallization temperatures of the α phase from the melt (T_c), and the melting transition temperatures of the α phase ($T_{f\alpha}$) for the 1,2-diacyl-*sn*-glycerols are plotted against the acyl chain length in Figure 5a. The thermal data for the racemic 1,2-DGs from Howe and Malkin (1951) are plotted for comparison. Melting temperatures for the racemic 1,2-DGs are systematically 6 °C lower than those for the corresponding 1,2-DGs. Either all of Malkin's racemic DGs contained impurities which lowered the melting point 6 °C, or racemic 1,2-DGs have a lower melting point than optically active 1,2-DGs. In contrast, the C_{16} and C_{18} α-form melting points obtained in this study and by Howe and Malkin differed by only 1–2 °C. The greater difference in the melting temperatures of the β' form than in the α form can be understood due to more specific interactions in the β' form than in the α form. Comparison of the α-form melting enthalpies and the recrystallization enthalpies (Table I) shows that they are nearly identical, confirming that recrystallization to the α form occurred in all cases.

The enthalpy (ΔH) and entropy (ΔS) of melting of the β' and α phases from Table I were plotted against the carbon number of the acyl chain. Both enthalpy and entropy showed linear relationships with the carbon number of the acyl chain, and the equations for the lines are

$$\Delta H_{f\beta'} = 1.86 \text{ (carbon number)} - 2.46 \text{ kcal/mol}$$

$$\Delta H_{f\alpha} = 1.30 \text{ (carbon number)} - 6.54 \text{ kcal/mol}$$

$$\Delta S_{f\beta'} = 4.60 \text{ (carbon number)} + 6.06 \text{ cal/mol}^{-1}\text{ K}^{-1}$$

$$\Delta S_{f\alpha} = 3.30 \text{ (carbon number)} - 8.71 \text{ cal/mol}^{-1}\text{ K}^{-1}$$

Since there are two chains per molecule, the slopes must be divided by 2 to get the ΔH and ΔS per $-CH_2-$. Thus, the ΔH per $-CH_2-$ in the β' to melt transition is 0.93 kcal and for the α to melt is 0.65 kcal. The corresponding ΔS values are 2.30 and 1.65 cal K^{-1} $(-CH_2-)^{-1}$. These values are very similar to those of other aliphatic molecules like alkanes and triacylglycerols (Small, 1986).

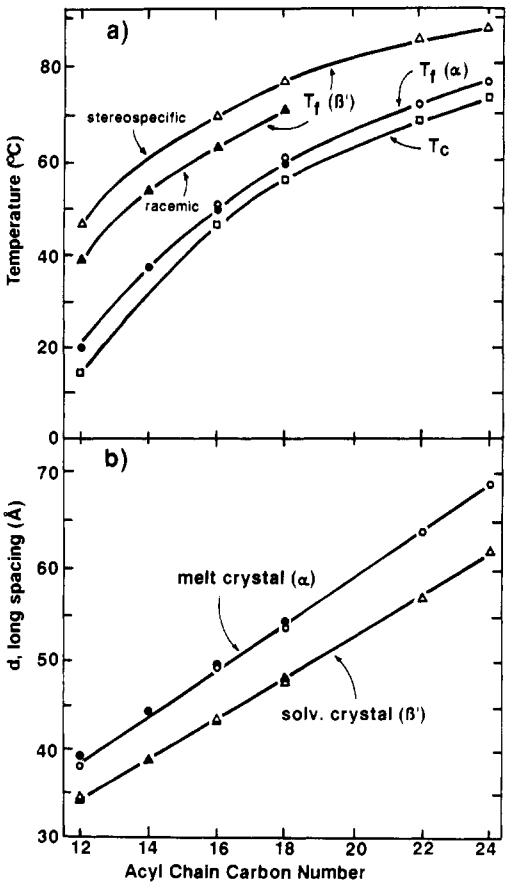

FIGURE 5: Thermal and X-ray diffraction data of 1,2-diacyl-*sn*-glycerols. (a) Melting temperatures $T_{f\beta'}$ and $T_{f\alpha}$ (▲, ○) and recrystallization (T_c) temperatures of 1,2-diacyl-*sn*-glycerols plotted against the acyl chain carbon number. The data for racemic 1,2-diacylglycerols (▲, ●) (Howe & Malkin, 1951) are plotted for comparison. (b) Plot of the interplanar d spacing vs acyl carbon number for the α and β' forms of 1,2-diacyl-*sn*-glycerols (○, △). Data from Howe and Malkin (1951) for the α and β' forms of racemic diacylglycerols are also plotted (●, ▲). A line drawn by least-squares fit through at least three 0,0,1 reflections (for each compound, data from Tables II and III) of the α and β' phases of 1,2-DG gave the equations $\alpha = (2.54 \pm 0.034)$(carbon number) + (7.88 ± 0.68) and $\beta' = (2.24 \pm 0.014)$(carbon number) + (7.69 ± 0.26). The slopes gave 2.54 Å and 2.24 Å/2 carbons in α and β', respectively. The chain tilt calculated from the slope gave 90° and 62° from the base methyl plane for the α and β' phases, respectively. The thickness of the glycerol region (two glycerol molecules) obtained from the equations is 7.9 and 7.7 Å for the α and β' forms, respectively.

The strong wide-angle diffractions at ca. 1/4.3, 1/4.0, and 1/3.8 Å^{-1} (Table II) for the hexane-crystallized 1,2-DGs indicate a β'-subcell packing arrangement. The single-crystal structure of the stable form of 1,2-diacyl-*sn*-glycerol (Pascher et al., 1981) showed an orthorhombic perpendicular subcell (β') with the acyl chains at the 1- and 2-positions packed in a hairpin configuration. Howe and Malkin (1951) observed β' short spacings for racemic 1,2-DG. However, they called this stable structure a "β-form". Kodali et al. (1984) mistakenly suggested the 1,2-dipalmitoyl-*sn*-glycerol solvent-crystallized form was β, based on the presence of a medium-intensity short spacing at 1/4.42 Å^{-1}. We now know that 1,2-diacyl-*sn*-glycerols have not been observed in a β form, which consists of a triclinic parallel subcell and a characteristic strong 1/4.6 Å^{-1} diffraction. Using infrared spectroscopy we

confirmed the solvent-crystallized form of 1,2-DG packed in an orthorhombic perpendicular subcell based on the splitting of methylene bending (1470 cm^{-1}) and rocking (720 cm^{-1}) absorptions (unpublished results), similar to the other long acyl chain containing glycerol derivatives (Kodali et al., 1989a,b).

Rapid cooling of the melt of C_{12}, C_{16}, and C_{18} 1,2-DGs crystallized to a hexagonally packed α form, characterized by a single strong 4.1 Å reflection (Table III). This form is very stable and transforms to a β' form at the α-form melting temperature (Figure 4a–c). Upon rapid cooling, the C_{22} and C_{24} 1,2-DGs crystallized to a sub-α form with wide-angle diffraction at ca. 4.1 and 3.8 $Å^{-1}$. This "sub-α" form transforms to an α form at temperatures well below $T_{f\alpha}$ (Figure 4d). The small broad endothermic events (<2 kcal/mol) at 19 and 30 °C for the C_{22} and C_{24} DGs (Figure 2) correspond to the sub-α to α transition.

The wide-angle diffraction indicates that the sub-α form contains pseudohexagonally packed chains. The long spacings of the sub-α and α forms are essentially the same, indicating that there is no tilt change along the long axis, but the subcell structure along the short axis of the acyl chains is changed. The transition from a low-temperature pseudohexagonal packing to a higher temperature true hexagonal packing is well characterized [for a review, see Small (1984, 1986)] It is known to occur in the $L_{\beta'}$ to $P_{\beta'}$ transition in hydrated synthetic phospholipids (Janiak et al., 1976) and in the rotator (α) phase of certain odd-carbon-numbered normal alkanes (Doucet et al., 1981; Small, 1986). Similarly, the long acyl chain 1,2-diacyl-*sn*-glycerols exhibit a pseudohexagonal to hexagonal chain packing transition. All these transitions are of low enthalpy (<2 kcal/mol). Racemic 1,2-dipalmitoylglycerol on prolonged storage well below the melting temperature was reported to form two modifications of the α (hexagonally packed chains) phase (Craievich et al., 1978). The first, called $L_{\beta'}$, retained hexagonally packed chains, but the chain axis was tilted a few degrees from normal to the layer plane. The second occurring at a lower temperature, L_r, was tilted and had a distorted hexagonal chain lattice like the sub-α phase found in this study.

This type of sub-a phase, based on the wide-angle diffraction pattern (ca. 4.2 and 3.8 Å), has been observed for some triacylglycerols, first in 1-palmitoyl- and 1-stearoyldibehenoylglycerols (Jackson & Lutton, 1950) and then in tristearoylglycerol below −50 °C (Chapman, 1962). The pseudohexagonal lattice present in the sub-α phase is less ordered but similar to the packing of the orthorhombic perpendicular subcell of the β' phase. IR spectral analysis also indicated a β'-subcell type for tristearoylglycerol in the sub-α phase at −50 °C (Chapman, 1962).

The stability of the α-phase increased with the acyl chain length. In the case of C_{12} 1,2-DG, the α- to β'-phase conversion is very facile; as shown in Figure 2, it is exothermic. In the case of C_{16} and C_{18} DGs, the α phase is quite stable if stored much below its melting temperature. However, if they are incubated near the α melting temperature, as is shown in Figure 3 (for C_{16} DG), the nucleation and growth of the β' phase occur. In C_{22} and C_{24}, the stability of the α phase increased substantially. In fact, in C_{24}, we have not observed any β' phase after it is stored for 5 months at 0 °C in the sub-α phase. However, if the newly formed α phase of C_{24} DG is reheated immediately, nucleation and growth of a small amount of β' phase are observed. Therefore, the stability of the α phase is governed by the chain length and incubation temperature. As the incubation time is increased, especially at higher temperatures, the problems of acyl migration (Kodali et al., 1990) limit the interpretation of results.

A plot of the length of the interplanar *d* spacing vs the number of carbons in the acyl chain from hexane-crystallized 1,2-DGs is shown in Figure 5b, lower line. Long spacing data from the work of Howe and Malkin (1951) are also plotted for comparison and are in reasonable agreement. From the single-crystal structure of 1,2-dilauroyl-*sn*-glycerol, Pascher (1981) reported the lengths of the unit-cell *c* axis to be 34.2 Å, essentially identical with the *d*-spacing value of 34.4 Å reported here. A line drawn by the least-squares fit through the $d_{0,0,l}$ reflections given in Table II gave an equation: $\beta' = (2.24 \pm 0.014)(\text{carbon number}) + (7.69 \pm 0.26)$. The slope of the line, 2.24 Å/2 carbons, gives an acyl chain tilt of 62° from the base methyl plane. This angle of chain tilt is quite similar to that of 1,2-dilauroyl-*sn*-glycerol (63.5°) reported by Pascher et al. (1981). The intercept at zero carbons for this line gives ca. 7.7 Å, representing the distance normal to the base plane occupied by the two glycerols. A similar plot of *d* spacing vs acyl carbon number for the α form of 1,2-diacyl-*sn*-glycerols is shown in Figure 5b, top line. The equation obtained after drawing a line by least-squares fit through the data given in Table III gave the following equation: $\alpha = (2.54 \pm 0.034)(\text{carbon number}) + (7.88 \pm 0.68)$. Analysis of the slope yields a chain tilt of 90°, indicating that the hydrocarbon chains are perpendicular to the base plane. In the α phase, the intercept at zero carbons gives ca. 7.9 Å, corresponding to the distance occupied by the two glycerol moieties from either side of the bilayer. The intercepts of the lines for β' and α are not significantly different.

1,3-Diacylglycerols. Considerably more work on the physical properties of 1,3-DGs has been reported than for the 1,2-DGs. Early studies of the 1,3-DGs by Malkin et al. (1937) and Baur et al. (1949) revealed two polymorphic forms. The stable form crystallized from hexane has a 2 Å greater long spacing and 2 °C greater melting temperature than the melt-crystallized form. These findings are in reasonable agreement with the results obtained in this study for C_{16} and C_{18} 1,3-DGs. The melting temperatures of hexane-crystallized 1,3-dipalmitoylglycerol reported by Malkin (1937) (72.5 °C) and Baur (1949) (72.9 °C) were found to be lower than this study (74.9 °C), perhaps reflecting higher purity. The melting points for hexane-crystallized 1,3-distearoylglycerol are reported as 78, 78.2, and 78.4 °C by Malkin (1937) and Baur (1949) and in this work, respectively. Thermal or X-ray diffraction pattern changes indicating a structural transition from the lower melting form to the higher melting form were not seen during heating of 1,3-DGs in this study.

The average *d* spacings for saturated 1,3-DGs reported in the earlier studies by Malkin (1937) and Baur (1949) are in reasonable agreement with each other and with values obtained here. Two sets of long spacings differing by about 2 Å correspond to the hexane-crystallized forms. The higher melting hexane-crystallized form has the greater long spacings. The long spacings of 1,3-DG are plotted against the acyl carbon number in Figure 6.

The single-crystal structure of bromine-substituted 1,3-diacylglycerol of 11-bromoundecanoic acid (Hybl & Dorset, 1971) shows an interplanar spacing of about 54.5 Å. This value does not even approximate the powder diffraction *d* spacings of 37.5 or 33.5 Å reported for 1,3-dilauroylglycerol by Malkin (1937) or Baur (1949). Nor are the single-crystal and powder diffraction *d* spacings multiples of each other, ruling out the possibility that the $d_{0,0,l}$ reflection is absent in the powder diffraction data. This indicates that the 1,3-dilauroylglycerol is not isostructural with bromine-substituted

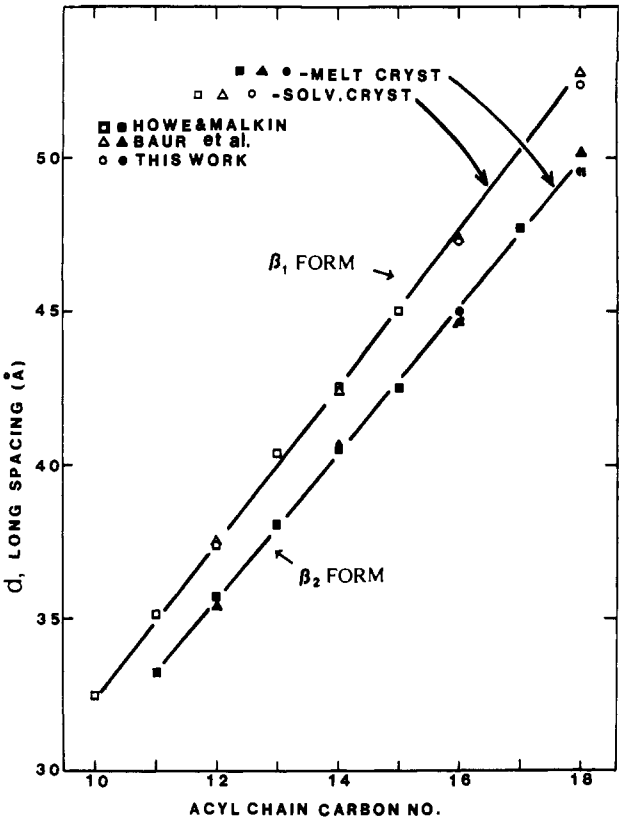

FIGURE 6: Plot of the interplanar *d* spacings vs carbon number of 1,3-diacylglycerols. The data from Howe and Malkin (1951) and Baur et al. (1949) are also plotted for comparison. Straight lines drawn by least-squares fit through the long spacing data for the β_1 and β_2 forms of 1,3-DG of Howe and Malkin (1951), Baur et al. (1949), and this work gave the equations $\beta_1 = (2.48 \pm 0.03)$(carbon number) + (7.78 ± 0.44) and $\beta_2 = (2.38 \pm 0.03)$(carbon number) + (6.88 ± 0.44). The acyl chain tilts calculated from the slope for the solvent-crystallized, β_1 form and the melt-crystallized β_2 form are 77.5° and 69.5°, respectively.

1,3-diacylglycerol of 11-bromoundecanoic acid. A greater chain tilt is probably required for the bromine-substituted DG in order to accommodate the bulky bromine atom. Straight lines are drawn through the β_1 and β_2 long spacing data from Howe and Malkin (1951), Baur (1949), and this work gave the equations:

$$\beta_1 = (2.48 \pm 0.029)(\text{carbon number}) + (7.78 \pm 0.44)$$

$$\beta_2 = (2.38 \pm 0.030)(\text{carbon number}) + (6.88 \pm 0.44)$$

Assuming that a unit cell contains one set of diametrically opposed and extended chains, an acyl chain tilt of 77.5° for the hexane-crystallized form and 69.5° for the melt-crystallized form can be calculated. However, the angle of tilt and increment in long spacing could be satisfied by other conformations. For example, the 1 and 3 chains may lie next to each other with two DG molecules contained in the unit cell. The thickness of the glycerol region obtained from the intercept at zero acyl carbons for these compounds is approximately 7.8 and 6.9 Å for β_1 and β_2, respectively. These values are not significantly different. A definitive single-crystal study of 1,3-diacylglycerol is needed to understand and compare the precise molecular packing in the glycerol region of 1,3-DG with 1,2-DG.

In summary, the molecular packing of naturally occurring 1,2-diacyl-*sn*-glycerols with saturated acyl chains has been examined and compared with 1,3-diacylglycerols. The polymorphic behavior of 1,2-diacyl-*sn*-glycerols as typified by C_{16} and C_{24} is schematically represented in Figure 7. The most

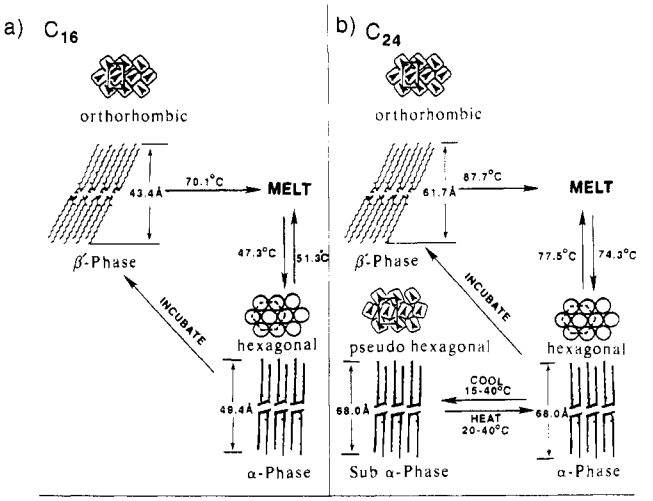

FIGURE 7: Schematic representations of the polymorphic behavior of 1,2-diacyl-*sn*-glycerols as exemplified by 1,2-dipalmitoyl-*sn*-glycerol (C_{16}) and 1,2-dilignoceroyl-*sn*-glycerol (C_{24}) are shown. The C_{16} behavior is typical for C_{12}–C_{18} 1,2-DGs. The polymorphism of C_{22} is similar to C_{24}. The subcell of each polymorph is represented on the top.

stable crystal form of 1,2-DG obtained from the solvent of crystallization packed in an orthorhombic perpendicular subcell (β' phase) with a chain tilt of 62° and melts to an isotropic liquid on heating. In these compounds, a metastable polymorph with a hexagonal subcell (α phase) and the chains normal to the basal methyl plane is formed on cooling the isotropic liquid. This α phase on incubation transforms into the β' phase. However, in C_{22} and C_{24}, the α phase can be reversibly converted to a sub-α phase with an orthorhombic perpendicular type subcell, on further cooling. In contrast, the packing of 1,3-DG exhibits, two β forms with a triclinic parallel subcell and a slight change in the chain tilt between the two forms.

ACKNOWLEDGMENTS

We thank David Atkinson for helpful discussion concerning the X-ray diffraction experiments. We also thank Balaji Bhyravabhatla and Charles Hastings for technical assistance and Margaret Gibbons for typing the manuscript.

Registry No. C_{12} DG, 60562-15-4; C_{16} DG, 30334-71-5; C_{18} DG, 10567-21-2; C_{22} DG, 129940-06-3; C_{24} DG, 129872-29-3; dimethylboron bromide, 5158-50-9.

REFERENCES

Baur, F. J., Jackson, F. L., Kolp, D. G., & Lutton, E. S. (1949) *J. Am. Chem. Soc. 71*, 3363–3366.

Bentley, P. H., McCrae, W. (1970) *J. Org. Chem. 35*, 2082–2083.

Carter, M. G. R., & Malkin, T. (1947) *J. Chem. Soc.*, 554–558.

Chapman, D. (1962) *Chem. Rev. 62*, 433–456.

Craievich, A. F., Levelut, A. M., Lambert, M., & Albon, N. (1978) *J. Phys. 39*, 377–388.

Daubert, B. F. & Lutton, E. S. (1947) *J. Am. Chem. Soc. 69*, 1449–1451.

Daubert, B. F., & Sidhu, S. S. (1948) *J. Am. Chem. Soc. 70*, 1848–1849.

Dorset, D. (1974) *Chem. Phys. Lipids 13*, 133–140.

Dorset, D. L., Pangborn, W. A., Hancock, A. J., & Lee, I. S. (1978) *Z. Naturforsch., C: Biosci. 33*, 39.

Dorset, D. L., & Pangborn, W. A. (1988) *Chem. Phys. Lipids 48*, 19–28.

Doucet, J., Denicolo, I., & Craievich, A. (1981) *J. Chem. Phys. 75*, 5125–5127.
Franks, A. (1958) *Br. J. Appl. Phys. 9*, 349–352.
Ganong, B. R., Loomis, C. R., Hannun, Y. A., & Bell, R. M. (1986) *Proc. Natl. Acad. Sci. U.S.A. 83*, 1184–1188.
Gros, A. T., & Feuge, R. O. (1957) *J. Am. Oil Chem. Soc. 34*, 239–244.
Howe, R. J., & Malkin, T. (1951) *J. Chem. Soc.*, 2663–2667.
Hybl, A., & Dorset, D. (1971) *Acta Crystallogr. B27*, 977–986.
IUPAC–IUB Commission on Biochemical Nomenclature (1977) *Eur. J. Biochem. 79*, 11–21.
Jackson, F. L., & Lutton, E. S. (1950) *J. Am. Chem. Soc. 72*, 4519–4521.
Janiak, M. J., Small, D. M., & Shipley, G. G. (1976) *Biochemistry 15*, 4575–4580.
Kodali, D. R., Atkinson, D., Redgrave, T. G., & Small, D. M. (1984) *J. Am. Oil Chem. Soc. 61*, 1078–1084.
Kodali, D. R., Atkinson, D., & Small, D. M. (1989a) *J. Dispersion Sci. Technol. 10*, 393–440.
Kodali, D. R., Atkinson, D., & Small, D. M. (1989b) *J. Phys. Chem. 93*, 4683–4691.
Kodali, D. R., Tercyak, A., Fahey, D. A., & Small, D. M. (1990) *Chem. Phys. Lipids 52*, 163–170.
Larsson, K. (1963) *Acta Crystallogr. 16*, 741–748.
Lok, C. M., & Ward, J. P. (1986) *Chem. Phys. Lipids 39*, 19–29.
Malkin, T., Shurbagy, M. R., & Meara, M. L. (1937) *J. Chem. Soc.*, 1409–1413.
Nishizuka, Y. (1986) *Science 233*, 305–312.
O'Connor, R. T., DuPre, E. F., & Feuge, R. O. (1955) *J. Am. Oil Chem. Soc. 32*, 88–93.
Pascher, I., Sundell, S., & Hauser, H. (1981) *J. Mol. Biol. 153*, 791–806.
Rando, R. R., & Young, N. (1984) *Biochem. Biophys. Res. Commun. 122*, 818–823.
Sekar, M. C., & Hokin, L. E. (1986) *J. Membr. Biol. 89*, 193–210.
Serdarevich, B. (1967) *J. Am. Oil Chem. Soc. 44*, 381–393.
Small, D. M. (1984) *J. Lipid Res. 25*, 1490–1500.
Small, D. M. (1986) The Physical Chemistry of Lipids from Alkanes to Phospholipids, in *Handbook of Lipid Research* (Hanahan, D., Ed.) Vol. 4, pp 1–672, Plenum Press, New York.

Heterologous Expression of Active Thymidylate Synthase–Dihydrofolate Reductase from *Plasmodium falciparum*†

Worachart Sirawaraporn,‡ Rachada Sirawaraporn,‡ Alan F. Cowman,§ Yongyuth Yuthavong,‡ and Daniel V. Santi*,‖

Department of Biochemistry, Faculty of Science, Mahidol University, Bangkok 10400, Thailand, The Walter and Eliza Hall Institute of Medical Research, Victoria 3050, Australia, and Department of Biochemistry and Biophysics and Department of Pharmaceutical Chemistry, University of California, San Francisco, California 94143-0448

Received July 19, 1990; Revised Manuscript Received October 3, 1990

ABSTRACT: The coding sequence of the bifunctional thymidylate synthase–dihydrofolate reductase (TS–DHFR) from a moderately pyrimethamine-resistant strain (HB3) of *Plasmodium falciparum* was assembled in a pUC expression vector. The coding sequence possesses unique *Nco*1 and *Xba*1 sites which flank 243 bp of the DHFR gene that include all point mutations thus far linked to pyrimethamine resistance. Wild-type (3D7) and highly pyrimethamine-resistant (7G8) TS–DHFRs were made from this vector by cassette mutagenesis using *Nco*1–*Xba*1 fragments from the corresponding cloned TS–DHFR genes. Catalytically active recombinant TS–DHFRs were expressed in *Escherichia coli*, albeit at low levels. Both TS and DHFR coeluted upon gel filtration and copurified upon affinity and anion exchange chromatography. Gel filtration and SDS–PAGE indicated that the enzyme was a dimer with identical 67-kDa subunits, characteristic of protozoan TS–DHFRs. Amino-terminal sequencing gave 10 amino acids which perfectly matched the sequence predicted from the nucleotide sequence. The recombinant TS–DHFR was purified to homogeneity by 10-formylfolate affinity chromatography followed by Mono Q FPLC. The inhibition properties of pyrimethamine toward the purified recombinant enzymes show that the point mutations are the molecular basis of pyrimethamine resistance in *P. falciparum*.

In most organisms, thymidylate synthase (TS) and dihydrofolate reductase (DHFR) are separate, monofunctional enzymes. DHFR is usually a monomer of about 20 kDa (Blakley, 1984), and TS is a dimer of identical subunits of about 35 kDa each (Santi, & Danenberg, 1984). However, in protozoa, the enzymes exist on the same 55–70-kDa polypeptide chain, with the DHFR domain at the amino terminus and TS at the carboxy terminus, separated by a junction peptide. The native bifunctional protein is comprised of two such subunits (Ivanetich & Santi, 1990).

The TS–DHFR[1] of *Plasmodium falciparum* is one of the

† This work was supported by the TDR/RF Joint Venture Programme and NIH Grant AI19538. W.S. is a recipient of a L. W. Frohlich Research Fellowship. A.F.C. is supported by a Wellcome Australian Senior Research Fellowship.

* To whom correspondence should be addressed.
‡ Mahidol University.
§ The Walter and Eliza Hall Institute of Medical Research.
‖ University of California.

[1] Abbreviations: TS–DHFR, thymidylate synthase–dihydrofolate reductase; H_2folate, 7,8-dihydrofolate; H_4folate, tetrahydrofolate; CH_2-H_4folate, 5,10-methylenetetrahydrofolate; FdUMP, 5-fluoro-2′-deoxyuridine 5′-monophosphate; MTX, methotrexate; PVDF, poly(vinylidine difluoride); SDS–PAGE, sodium dodecyl sulfate–polyacrylamide gel electrophoresis; Pyr, pyrimethamine; Amp, ampicillin; ON, oligonucleotide; nt, nucleotide; TES, 2-[[tris(hydroxymethyl)methyl]amino]ethanesulfonate.

0006-2960/90/0429-10779$02.50/0